J. Phycol. **53,** 85–94 (2017)

DOI: 10.1111/jpy.12480

ABIOTIC INFLUENCES ON BICARBONATE USE IN THE GIANT KELP, *MACROCYSTIS PYRIFERA*, IN THE MONTEREY BAY[1]

Sarah Tepler Drobnitch[2]

Department of Ecology and Evolutionary Biology, University of California, Santa Cruz, Santa Cruz, California 95060, USA

Kerry Nickols

School of Natural Sciences, California State University, Monterey Bay, Seaside, California 93955, USA

and Matthew Edwards

Department of Biology, San Diego State University, San Diego, California 92101, USA

In the Monterey Bay region of central California, the giant kelp *Macrocystis pyrifera* experiences broad fluctuations in wave forces, temperature, light availability, nutrient availability, and seawater carbonate chemistry, all of which may impact their productivity. In particular, current velocities and light intensity may strongly regulate the supply and demand of inorganic carbon (Ci) as substrates for photosynthesis. *Macrocystis pyrifera* can acquire and utilize both CO_2 and bicarbonate (HCO_3^-) as Ci substrates for photosynthesis and growth. Given the variability in carbon delivery (due to current velocities and varying [DIC]) and demand (in the form of saturating irradiance), we hypothesized that the proportion of CO_2 and bicarbonate utilized is not constant for *M. pyrifera*, but a variable function of their fluctuating environment. We further hypothesized that populations acclimated to different wave exposure and irradiance habitats would display different patterns of bicarbonate uptake. To test these hypotheses, we carried out oxygen evolution trials in the laboratory to measure the proportion of bicarbonate utilized by *M. pyrifera* via external CA under an orthogonal cross of velocity, irradiance, and acclimation treatments. Our Monterey Bay populations of *M. pyrifera* exhibited proportionally higher external bicarbonate utilization in high irradiance and high flow velocity conditions than in sub-saturating irradiance or low flow velocity conditions. However, there was no significant difference in proportional bicarbonate use between deep blades and canopy blades, nor between individuals from wave-exposed versus wave-protected sites. This study contributes a new field-oriented perspective on the abiotic controls of carbon utilization physiology in macroalgae.

Key index words: **acclimation; acetazolamide; bicarbonate; *Macrocystis pyrifera*; microenvironment**

***Abbreviations*: ADCP, acoustic Doppler current profiler; AZ, acetazolamide; C_i, inorganic carbon; DIC, dissolved inorganic carbon; EBU, external bicarbonate utilization**

The organisms that inhabit nearshore and intertidal marine ecosystems must cope with fluctuations in wave forces, temperature, light availability, nutrient availability, and seawater carbonate chemistry. Kelps (Laminariales), which are critically important foundation species (sensu Dayton 1972) and ecosystem engineers (sensu Jones et al. 1994, Ellison et al. 2005), experience this variability in shallow temperate waters around the world. For example, kelp forests along the central coast of California experience water temperature fluctuations of 4°C on a daily basis due to tidal bores and internal waves propagating inshore, and seasonal fluctuations of up to 7°C due to upwelling vs. relaxed oceanographic conditions (Storlazzi et al. 2003, Woodson et al. 2007). Irradiance varies with depth—for example, irradiance at 12 m depth is only ~10% of surface values and macroalgal canopies further reduce irradiance at depth by 75% (Gerard 1984, Edwards 1998). Wave force and current velocities also vary seasonally and geographically; kelp forest communities at exposed sites frequently experience current velocities in excess of 30 cm s^{-1} while velocities lower than 2 cm s^{-1} occur in nearby protected embayments (Gaylord et al. 2003, Storlazzi et al. 2003).

The giant kelp, *Macrocystis pyrifera* C.Agardh, has a worldwide distribution on temperate rocky coastlines (Graham et al. 2007), and successfully tolerates a broad range of temperatures, nutrient availability, light availability, and hydrodynamic stress (Gerard 1982, Alonso Vega et al. 2005, Graham et al. 2007, Schiel and Foster 2015, Carr and Reed 2016). Furthermore, *M. pyrifera* is known to acclimate to these abiotic factors by altering its sporophyte morphology and photosynthetic physiology (Brostoff 1988, Kopczak et al. 1991, Utter and Denny 1996, Colombo-Pallotta et al. 2006, Stewart et al. 2009,

[1]Received 7 April 2016. Accepted 2 September 2016.
[2]Author for correspondence: e-mail stepler@ucsc.edu.
Editorial Responsibility: C. Amsler (Associate Editor)

Hurd and Pilditch 2011). We lack, however, a clear understanding of how environmental factors impact carbon acquisition physiology in *M. pyrifera* and other large brown macroalgae. Recent work has focused on the effects of variable pH environments on carbon acquisition (Brown et al. 2014, Fernández et al. 2015), but we have little information regarding the effects of variable irradiance and current velocities on carbon uptake dynamics in *M. pyrifera*.

Macrocystis pyrifera can utilize both CO_2 and HCO_3^- (bicarbonate) as substrates for photosynthesis (PS) and growth. These two species of inorganic carbon differ strongly in availability and ease of uptake by photosynthetic organisms at current ocean pH. CO_2 is a small nonpolar molecule that diffuses easily across cell membranes and requires no costly active uptake mechanism, but comprises only 1% of seawater Ci at pH 8.1. In contrast, bicarbonate is strongly polar and requires active transport or external catalysis to CO_2 to be utilized as a photosynthetic substrate, yet is abundantly available (91% of Ci) (The Royal Society 2005). Consequently, the ability to utilize bicarbonate as a substrate in photosynthesis is beneficial but may not always be cost-effective for marine algae (Raven et al. 2014).

Environmental variation in irradiance and current velocities may strongly affect patterns of carbon uptake. Current velocity can control supply of inorganic carbon (Ci) to *M. pyrifera*. Low current velocities (<3 cm $\cdot$ s^{-1}) have been shown to induce boundary layer formation that limits the nutrient influx to and efflux from kelp blades (Wheeler 1980), whereas velocities greater than 3 cm $\cdot$ s^{-1} saturate gas exchange rates. Irradiance, on the other hand, regulate Ci demand. High irradiance experienced by canopy blades stimulates increased photosynthesis (Sharkey et al. 1986) and demand for Ci unlike that experienced by deeper understory blades.

In this study, we ask the following questions: Does *M. pyrifera* use a constant proportion of bicarbonate relative to CO_2, or does relative bicarbonate utilization vary? Furthermore, is the proportion of bicarbonate use influenced by abiotic conditions that alter Ci supply (current velocities) and/or photosynthetic demand (irradiance levels)? Finally, do local populations of *M. pyrifera* display acclimation of carbon uptake physiology to local physical conditions?

If *M. pyrifera* upregulates bicarbonate uptake in response to low ambient [Ci], we would hypothesize that in low flow velocities (diffusion-limited Ci supply) and high irradiance (high photochemical demand), *M. pyrifera* would exhibit the highest proportional bicarbonate use. On the other hand, we would hypothesize that *M. pyrifera* would utilize the smallest proportion of bicarbonate when photosynthesizing in high flow velocities and low irradiance (saturating Ci supply coupled with low photochemical demand). Previous studies have demonstrated that bicarbonate utilization is up- and down-regulated by light-mediated processes, and that bicarbonate utilization is down-regulated in very high [Ci] (Johnston and Raven 1990, Kubler and Raven 1995, Zou et al. 2003, Mcginn et al. 2004, Raven and Hurd 2012, Fernández et al. 2015, Hennon et al. 2015, Young et al. 2015). However, no study has observed induction of increased bicarbonate uptake in response to exposure to low [Ci]. If low ambient [Ci] does not actively up-regulate bicarbonate utilization, low flow velocities would instead limit the supply of both CO_2 and bicarbonate, resulting in proportionally lower bicarbonate utilization relative to tissues photosynthesizing in high flow velocities.

We further hypothesized that *M. pyrifera* blades acclimate their bicarbonate utilization mechanism, thus altering proportional bicarbonate use, in response to microhabitats characterized by consistent high and low irradiance and flow velocity levels. If acclimated, consistently light-limited blades should exhibit lower proportional bicarbonate use than light-replete canopy blades when exposed to high irradiance in the laboratory. Similarly, if blades from high wave exposure habitats were acclimated to greater ambient current velocities and thus higher rates of gas exchange, they should exhibit lower ability to utilize bicarbonate when incubated in low current velocities as compared with blades accustomed to low flow environments.

To evaluate these hypotheses, we carried out a set of laboratory experiments to estimate the relative utilization of bicarbonate in support of photosynthesis as a function of orthogonal combinations of irradiance, flow velocity, and blade origin treatments. To assess relative utilization of bicarbonate versus CO_2, we used acetazolamide (AZ), a potent inhibitor of the enzyme carbonic anhydrase (CA). AZ, which must be dissolved in NaOH, and thus acts as a slight carbonate buffer, inhibits external utilization of bicarbonate both via CA activity and acidification of the extracellular space (Drechsler et al. 1993, Larsson and Axelsson 1999, Klenell et al. 2004, Mercado et al. 2006). When actively photosynthesizing tissue is inhibited by AZ, removing their external utilization of bicarbonate, photosynthetic rates decrease. These lower, inhibited photosynthetic rates are thus a measure of metabolism supported only by CO_2 uptake and an unknown fraction of active bicarbonate uptake (via anion-exchange channels, which do not respond to AZ).

METHODS

Experimental approach. To test our predictions of carbon uptake of *M. pyrifera* to in response to the levels of irradiance and flow velocity experienced in the field, we measured the contribution of external bicarbonate utilization (EBU) to photosynthetic rates in two experiments. In 2014, we measured the effect of irradiance, flow velocity, and blade origin from different irradiance habitats on the proportion of bicarbonate uptake during photosynthesis. We orthogonally tested the separate and combined effects of two levels of irradiance (1,000

or 80 μmol photons · m^2 · s^{-1}), two levels of flow velocity (30 or 4.5 cm · s^{-1}), and two levels of blade origin (blades from the surface or 10 m depth) on uninhibited photosynthesis and acetazolamide-inhibited photosynthesis rates (AZPS). Since AZ inhibits the utilization of bicarbonate via extracellular catalysis, photosynthesis represents full CO_2 + bicarbonate utilization and AZPS represents only CO_2 uptake and an unknown proportion of active bicarbonate uptake. Biologically relevant saturating and nonsaturating irradiance levels were selected by consulting previous studies of *M. pyrifera* in the field (Stewart et al. 2009, Edwards and Kim 2010).

In 2015, we again measured the effect of irradiance and flow velocity, but examined the effect of blade origin from different wave exposure habitats on relative bicarbonate uptake during photosynthesis. We tested orthogonally for the separate and combined effects of two levels of irradiance (800 or 100 μmol photons · m^2 · s^{-1}), two levels of flow velocity (10 or 3 cm · s^{-1}), and two levels of blade origin (from protected or exposed hydrodynamic populations) on photosynthesis and AZPS. Flow velocity treatments were lowered in 2015 to reflect velocities frequently encountered by blades at the Hopkins Marine Station, where we carried out detailed depth-stratified current velocity measurements (see Results). Light levels were slightly different in 2015, but remained below and above the irradiance threshold for PS (200 μmol photons · m^2 · s^{-1}) in *M. pyrifera* (Gerard 1984).

Collection of M. pyrifera *fronds for photosynthesis experiments.* To explore the possibility that the carbon uptake physiology of *M. pyrifera* is acclimated to high and low irradiance microenvironments, we collected individual frond segments from sporophytes growing in the McAbee kelp bed (Monterey Bay, California; N 36.61485, W 121.89706) in March 2014. Light-replete frond segments containing at least six entire and nonepiphytized blades were collected 2 m distal to the apical scimitar of the frond. Light-limited frond segments were collected at 10 m depth from mature fronds that reached the surface. Each frond segment was taken from a separate sporophyte. These segments were transferred in a cooler of cold seawater back to Long Marine Laboratory (University of California, Santa Cruz). Therefore, each blade of each segment was trimmed to a length of 35 cm to fit in the working section of the respirometer and held for 24–72 h indoors in a flow-through seawater table away from a shaded window (light level ~5 μmols photons · m^{-2}).

To explore the possibility that the carbon uptake physiology of *M. pyrifera* is acclimated to high and low wave exposure habitats, we collected meter-long segments from the surface fronds of wave-protected kelp beds (McAbee, Hopkins Marine Station, Stillwater Cove) and wave-exposed kelp beds (Otter Pt., Pt. Piños, and Sunset Pt.) in the Monterey and Carmel bays in February 2015 (coordinates in Table S1 in the Supporting Information). These sites represent the extremes of possible wave-exposed and wave-protected conditions in Central California, yet are located along a single peninsula. The exposed sites experience significantly higher wave heights and forces in empirical and modeled data sets (USGS SWAN wave force model, Table S1, one-tailed *t*-test, $P = 0.011$, df = 2.81, *t*-ratio = 4.63) (Graham et al. 1997, Figurski 2010, Erikson et al. 2014). While the relationship between wave exposure and unidirectional (current-driven) velocity magnitudes is complex and unknown for most of our sites, increased wave exposure is empirically associated with higher velocity magnitudes throughout the water column in a recent study near the Hopkins Marine Station kelp forest (Koweek et al. in review). In general, since high wave exposure sites in the Monterey Bay are also oriented toward the open ocean, we would expect unidirectional current velocities to increase with wave exposure at all our sites. After collection, frond segments were immediately transported to the NOAA SWFSC adjacent to Long Marine Lab, where they were trimmed and held in a shaded outdoor flow-through tank (maximum ~100 μmol photon · m^{-2}) for 24–72 h. During both study periods, filtered seawater ranged between 13°C and 16°C.

Oxygen evolution experiments. To measure photosynthetic rates of entire *M. pyrifera* blades in response to irradiance and velocity treatments, we carried out oxygen evolution experiments in a Loligo swim tunnel respirometer 10 L (Loligo Systems, Viborg, Denmark). While flow velocity is an important determinant of boundary layer thickness, studies have shown that blade structure and rugosity also strongly influence boundary layer thickness in *M. pyrifera* (Hurd and Pilditch 2011). Furthermore, while the use of tissue discs subsampled from entire blades is prevalent in recent studies, it is well established that there is significant variability in photosynthetic rates within single blades, and that tissue wounding impacts photosynthetic studies (Arnold and Manley 1985). Thus, we used the Loligo respirometer with a 10 L working volume instead of traditional BOD bottles to accommodate entire *M. pyrifera* blades. The respirometer was comprised of a sealed rectangular working section (40 × 10 × 10 cm) and collimator surrounded by a recirculating seawater jacket. The working section was fitted with a self-sealing silicone injection port and an oxygen sensor port. The oxygen meter (Firesting O_2, Pyro Science, Germany) was fitted with an optical sensor and thermocouple, and measured temperature-corrected dissolved oxygen concentrations once per second. The oxygen meter was calibrated daily. Rates of respiration and photosynthesis were calculated as the slope of linear decrease and increase, respectively, of the [O_2] in the sealed respirometer. Photosynthesis was stimulated by two artificial light fixtures (200 W sodium halide bulb in combination with a GE 65 W blue Plant Grow Light). When combined, the fixtures produced measurable light at all wavelengths relevant to photosynthesis (Fig. S1 in the Supporting Information).

For each oxygen evolution trial, a healthy, mature blade was chosen haphazardly from the collected *M. pyrifera* segments (after at least 24 h incubation) and tethered in the working section of the respirometer. The respirometer was then filled with 2 micron filtered seawater and sealed, and photosynthesis was measured in four phases. First dark respiration (R1) was measured under complete darkness using a custom fabric-draped shade box. Then uninhibited photosynthesis was measured under artificial light. After this, 3.3 mL of 25 mM AZ in 0.05 M NaOH (final concentration = 100 μM) was injected to inhibit external use of bicarbonate; with the light level unaltered, photosynthesis under this constraint (AZPS) was measured. Finally, the trial was completed with a second measurement of respiration (R2) in complete darkness. Each illuminated phase of measurement was carried out for 15–20 min, resulting in a maximum of 40 min of photosynthetic activity in 10 L of seawater. After oxygen measurements were completed, the kelp blade was refrigerated in the dark at 4°C and reserved for pigment extraction within 24 h. We conducted a set of controls for one full replicate of each Treatment (1, 2, 3, and 4) on light-acclimated blades by injecting 0.05 M NaOH solution instead of the NaOH-based AZ solution. These controls confirmed that (i) injection of this weak base had no impact on photosynthetic rates and (ii) AZ was responsible for observed reductions in photosynthetic rates post-injection.

The measurement of oxygen evolution is potentially problematic at very low flow velocities. Since we hypothesize that flow velocities less than 3 cm · s^{-1} may drive photosynthetic limitation via boundary layer formation, photosynthetically produced oxygen may be trapped in the boundary layer, delaying, or reducing detection in the bulk flow by the oxygen sensor. To qualitatively assess the completeness of fluid mixing in the respirometer, we injected saturated Rhodamine

B dye solution onto the blade at each flow treatment level. At 10 cm · s^{-1}, dye mixed almost immediately (<3 s). At 3 cm · s^{-1}, dye remained on the blade for much longer, but did eventually fully mix in ~30 s. Trials run at 3 cm · s^{-1} indeed generated much more variable oxygen evolution traces than trials run at 10 cm · s^{-1} and faster. Since, however, rates of oxygen production were integrated over several minutes, it is likely that O_2 sensor detected accurate levels of oxygen production for the two different flow velocities.

For each measurement period of the oxygen evolution trials (R1, photosynthesis [PS], AZPS, and R2), [O_2] data were trimmed by visual inspection to the most stable 2–5 min of measurement duration. The relationship between [O_2] and time (s) was always linear in these durations. Linear regression was then used to estimate the slope each measurement period in R (R Core Team, 2013). Gross photosynthesis was calculated as R1 + photosynthesis whereas AZ-inhibited gross photosynthesis was calculated as AZPS + R2. Photosynthetic rates were normalized to blade wet weight. To calculate the proportion of EBU during each trial, we used the following equation:

$$\text{Proportion EBU} = ((\text{PS} + \text{R1}) - (\text{AZ} + \text{R2}))/(\text{PS} + \text{R1})$$

Monitoring of seawater [Ci] during experimentation. Ci is highly variable along the coast of California (including the Monterey Bay) due to tidal, upwelling, and stratification events (Frieder et al. 2012, Kapsenberg and Hofmann 2016). In a representative kelp forest at the Hopkins Marine Station, pCO_2 ranges between 260 and 770 μatm at the benthos yearly (pH = 7.78–8.20, total scale), and between 175 and 540 μatm at the surface (pH = 7.92–8.33, total scale; Koweek et al. in prep.). Variation in pH, water temperature, and salinity are all driven by upwelling processes within the Monterey Bay, which has little to no freshwater input. During upwelling relaxation, temperatures range from 11°C to 16°C, whereas they drop significantly (9°C–10°C) during upwelling (Drake et al. 2005). Salinity varied between 33.1 and 33.9 on a yearly basis (Ward 2005).

To monitor for variation in seawater [Ci] supply at Long Marine Lab, water samples were collected at the start and end of a subsample of oxygen evolution trials in 2014 (16 runs), and for all trials in 2015. Water samples were fixed with 200 μL saturated $HgCl_2$ and stored in 120 mL borosilicate glass bottles sealed with parafilm at 4°C until total alkalinity (TA) and pH could be measured. To determine [DIC] of the seawater samples, we measured the pH and TA within 8 months of $HgCl_2$ fixation. pH was measured in triplicate on a spectrophotometer using the indicator dye m-cresol purple (pH of solution = 7.9 ± 0.01) in a temperature-controlled measurement cell set to 25°C. Absorbances of the dyed and undyed sample were measured at three wavelengths: a nonabsorbing wavelength (730 nm for m-cresol purple) and at the wavelengths corresponding to the absorption maxima of the base (I2–) and acid (HI–) forms of the dye, respectively (578 and 434 nm). TA was measured in duplicate or singly using open-cell titration with HCl on the Titrando automatic titrator (MetroOhm Inc. Herisau, Switzerland) in a jacketed flask maintained at 25°C. The titrator was calibrated daily with certified reference material from the Dickson Laboratory at the Scripps Institution of Oceanography. TA was calculated from the second (i.e., highest) integral endpoint calculated by the Tiamo (MetroOhm Inc.) software. TA and pH for each sample were then entered into the CO2SYS Excel macro (v.2, Pierrot et al. 2006) to calculate [DIC] and pCO_2 at 15°C (the temperature at which the oxygen evolution experiments were run). Boxplot distributions of pCO_2 and pH measurements for each experiment are presented in Figure S2 in the Supporting Information.

Measurement of pigment content in incubated blades. To assess possible local adaptation of tissue pigment content to our collection sites, relative pigment concentrations were measured within 24 h of each oxygen evolution trial. Fucoxanthin, chl *a*, and chl *c* were extracted from fresh (refrigerated) tissue discs (2.5 cm diameter) with acetone, methanol, and dimethyl sulfoxide in 30 mL glass test tubes capped with parafilm. Tissue discs were first extracted with dimethyl sulfoxide and water (4:1) on ice for 15 min; the disc was then transferred to a new test tube for further extraction with a 4:1:1 mixture of acetone, methanol, and water in a dark chamber for 2 h. Absorbance of extracts was measured on a ThermoScientific GENESYS 10S UV-VIS spectrophotometer (Waltham, MA, USA) at 665, 631, 582, and 480 nm and converted to g pigment per kg kelp tissue using the calculations detailed in Seely et al. 1972.

Measurement of within-kelp forest current velocity. The flow velocities that limit gas exchange in *M. pyrifera* blades are known from laboratory studies (Wheeler 1980), but we have no detailed knowledge of the velocities experienced by *M. pyrifera* within the water column of a mature kelp forest. To parameterize the unidirectional velocities used in our oxygen evolution experiments, we measured unidirectional background current velocities within a low wave exposure kelp forest.

Water column velocity was measured in July and October 2013 with a bottom-mounted acoustic Doppler current profiler (ADCP; 1,200 kHz; RD Instruments Poway, CA, USA). The instrument was deployed in the middle of a kelp bed offshore of Hopkins Marine Station in southern Monterey Bay, CA (36.6216 N, 121.90176 W) at a depth of 10 m. Instantaneous velocity measurements were recorded every 3 min in 0.5 m vertical bins that extended from ~1.5 m above the bottom to ~1.5 m below the surface. Velocity magnitudes were calculated as the square root of the sum of the east-west velocity component squared and the north-south velocity component squared. These velocity magnitudes quantitate the unidirectional background currents experienced by kelp plants, as they do not capture wave orbital velocity, oscillatory flow, or the movement of the kelp tissue itself relative to the adjacent water mass.

Statistical analysis. We removed outliers representing instrument or operator error from each photosynthetic rate data set using JMP Pro 12 (SAS Institute, Inc. Cary, NC, USA). Type I ANOVA was performed separately for each experiment (2014 and 2015) to test the hypothesis that light level, flow velocity, and blade origin influence the proportion of externally utilized bicarbonate used to support photosynthesis. We also tested for the interaction between irradiance and blade origin in 2014, and between flow velocity and blade origin in 2015. We did not test for any other interactions because they were not relevant to our hypotheses. The proportion of externally utilized bicarbonate was normally distributed, not binomial, and so we did not transform the data.

Gross photosynthetic rates were square root transformed for analysis to correct for slight non-normality and heteroscedasticity. In 2014, we performed a type I ANOVA to test for the fixed effects of irradiance, flow velocity, blade origin, and irradiance × blade origin on AZPS and photosynthesis as separate dependent variables. To account for the possible influence of fluctuating CO_2 concentrations in experimental seawater, we carried out a least squares regression analysis on a subset of our photosynthesis and AZPS data sets. In 2014, pCO_2 had no correlation with gross photosynthetic rates, whereas pCO_2 was significantly correlated with gross photosynthesis magnitude in 2015. Thus in 2015, we used an ANCOVA approach on PS and AZPS with pCO_2 as a continuous variable to examine the fixed effects of irradiance, flow velocity, blade origin (wave exposure), and the interaction between flow velocity and blade origin. Again, we did not test for any other interactions because they were not relevant to our hypotheses.

RESULTS

Measurement of flow velocities within a protected kelp forest. ADCP measurements indicated that unidirectional background current velocities slower than 3 cm · s^{-1} persistently occur in the protected Hopkins Marine Station kelp forest, especially at depth (5+ m deep). At 8.5 m depth, these low velocities occur continuously for 15 min for 40%–80% of each day (top two panels, Fig. 1 and Fig. S3 in the Supporting Information). Longer duration periods of slow flow also occur at depth, but less frequently; velocities slower than 3 cm · s^{-1} can occur continuously for 60 min 10%–40% of the time (bottom right panels, Figs. 1 and S3). These critically low flow velocities occur rarely, if at all, at the upper part of the water column (surface to 1.5 m depth, Fig. 1 and Fig. S3, top right). These data indicate that kelp at protected sites regularly experience currents that can limit gas exchange, but mostly near the seafloor. As such, kelp tissues that experience low flows also must experience low light; thus the experimental conditions in which kelp are photosynthesizing at high light levels but low flow levels (Treatment 3) are unlikely to occur in the field. Nonetheless, it was important to manipulate these two factors orthogonally to fully evaluate their relative effects on bicarbonate use.

Oxygen evolution experiments: Proportion of external bicarbonate uptake under irradiance and velocity treatments. In 2014, the mean proportion of photosynthesis supported by EBU clearly differed in response to irradiance exposure level, but not blade origin or flow velocity (ANOVA, Table 1; Fig. 2). Blades photosynthesizing at low irradiance levels (analogous to irradiance levels at 10 m depth beneath a full canopy) used only an average 27% ± 3.7% external bicarbonate whereas blades experiencing high irradiance (analogous to surface canopy conditions) used an average of 53% ± 3.8% external bicarbonate.

In 2015, irradiance and flow velocity both influenced the proportion of photosynthesis supported by EBU, but blade origin (differing exposure habitats) did not (ANOVA, Table 1; Fig. 3, blade origin not shown). Proportional EBU was reduced in low irradiance treatments (mean = 33% ± 3.4%) relative to high irradiance treatments (mean = 43% ± 3.7%). Kelp blades experiencing flows below 3 cm · s^{-1} (limiting Ci supply) used an average 30% ± 3.4% external bicarbonate whereas those blades experiencing flows of 10 cm · s^{-1} used an average 46% ± 3.7% external bicarbonate to support photosynthesis. There was no interaction between flow velocity and blade origin.

Oxygen evolution experiments: Patterns of gross photosynthesis in response to irradiance and velocity treatments in blades from different populations. In 2014, both AZ-inhibited (AZPS) and uninhibited photosynthetic rates varied as a function of blade origin (ANOVA, Table 2, Figs. S5 and S6 in the Supporting Information). Surface blades photosynthesized at greater rates (15.30 ± 0.105 μmols O_2 · g^{-1} FW · h^{-1}) than 10 m deep blades (12.16 ± 0.109 μmols O_2 · g^{-1} FW · h^{-1}). AZ inhibited photosynthesis was also much greater in surface

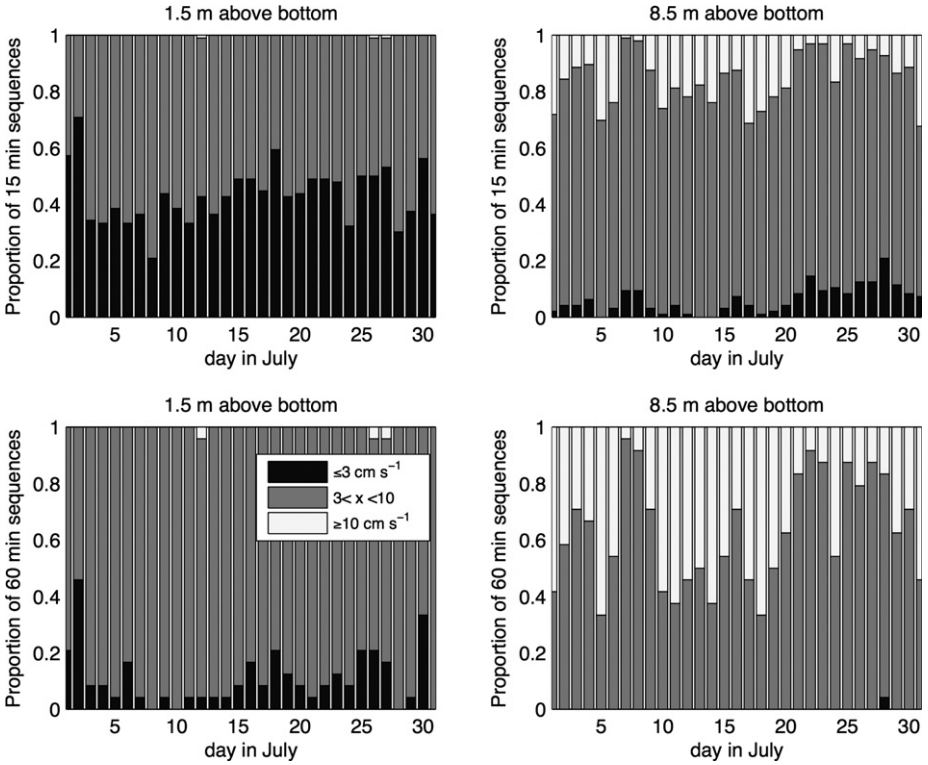

FIG. 1. Proportions of 15 min periods (A, B) and 60 min periods (C, D) each day in July 2013 when velocities were less than or equal to 3 cm · s^{-1} (dark blue), between 3 and 10 cm · s^{-1} (medium green) or greater than 10 cm · s^{-1} (light yellow) at the closest ADCP bin to the bottom (1.5 m above bottom; A, C) and the closest ADCP bin to the surface (8.5 m above bottom; B, D). October 2013 data can be found in Figure S3.

TABLE 1. Effect of experimental treatments on the fraction of photosynthesis supported by external bicarbonate utilization. ANOVA, df = 1.

Year	Fixed effect	*F*-ratio	*P* > *F*
2014	Blade origin (irradiance)	3.16	0.0873
2014	Light	23.12	<0.0001***
2014	Flow velocity	0.27	0.6103
2014	Blade origin × light	0.04	0.8413
2015	Blade origin (exposure)	0.04	0.8413
2015	Light	4.40	0.0436*
2015	Flow velocity	10.73	0.0025**
2015	Blade origin × flow velocity	0.05	0.822

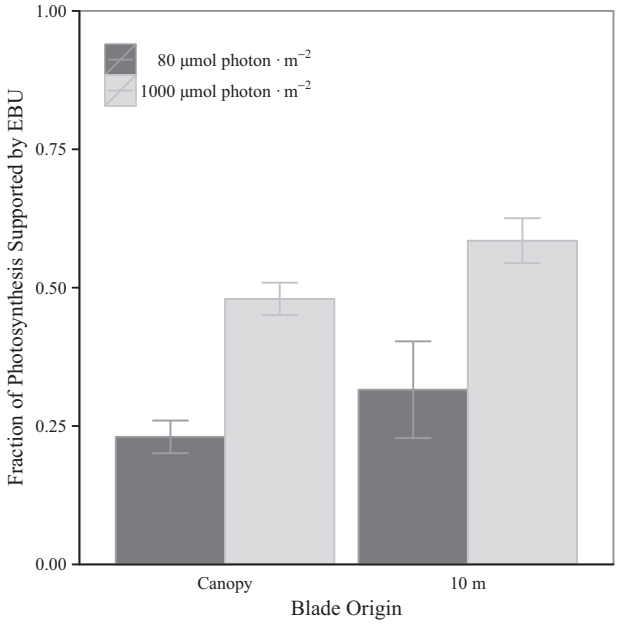

FIG. 2. Fraction of photosynthesis supported by external bicarbonate uptake as a function of irradiance level and blade origin (surface and 10 m). Fractions were calculated from rates of gross photosynthesis and AZPS from the 2014 experiment. Error bars represent SE.

blades (9.25 ± 0.107 μmols $O_2 \cdot g^{-1}$ FW $\cdot h^{-1}$) than 10 m deep blades (6.19 ± 0.110 μmols $O_2 \cdot g^{-1}$ FW $\cdot h^{-1}$, Fig. 4). As expected, high irradiance increased both photosynthesis ($P < 0.0001$) and AZPS ($P = 0.0173$) relative to the low irradiance treatment. There was a significant interaction of blade origin with irradiance treatment on photosynthesis ($P = 0.0101$) and AZPS ($P = 0.0256$); 10 m deep (light-limited) blades showed reduced photosynthesis in response to the high irradiance treatment but were indistinguishable from light-replete canopy blades under the low irradiance treatment. It is possible, therefore, that the light-limited blades expressed lower rates of photosynthesis under our high light treatment because of photoinhibition (Cabello-Pasini et al. 2000). pCO_2 was not correlated with photosynthesis or AZPS in our subsample of oxygen evolution trials (Least Squares Regression: Photosynthesis, $F_{15} = 0.4887$, $P = 0.496$; AZPS, $F_{15} = 0.2280$, $P = 0.6403$).

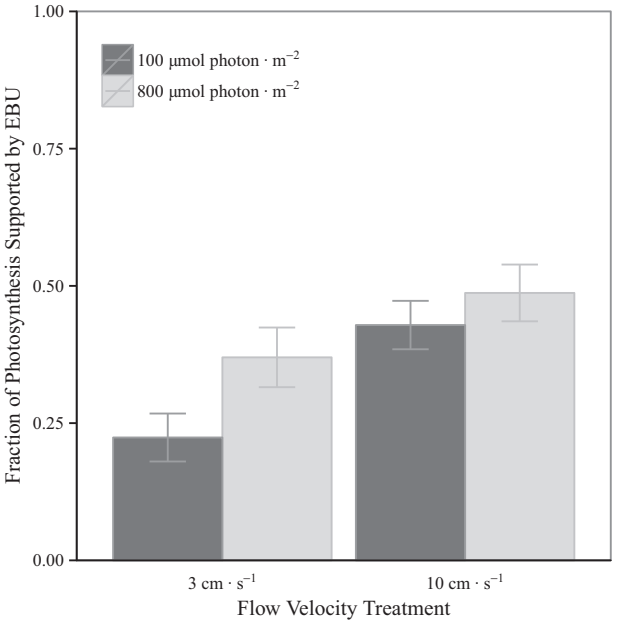

FIG. 3. Fraction of photosynthesis supported by external bicarbonate uptake as a function of irradiance level and flow velocity. Fractions were calculated from rates of gross photosynthesis and AZPS from the 2015 experiment. Error bars represent SE.

TABLE 2. Effect of experimental treatments on uninhibited photosynthesis (PS, square root transformed) or AZ-inhibited photosynthesis (AZPS, square root transformed). 2014 data: ANOVA, df = 1. 2015 data: ANCOVA, df = 1, continuous variable = pCO_2 of experimental incubation seawater. Asterisks denote significance levels. Graphical representation of mean photosynthesis and AZPS in response to these treatments can be found in Figures S5 and S6.

Data	Year	Fixed effect	*F*-ratio	*P* > *F*
PS	2014	Blade origin (irradiance)	7.88	0.0093**
PS	2014	Light	75.64	<0.0001***
PS	2014	Flow velocity	3.91	0.0588
PS	2014	Blade origin × Light	7.70	0.0101*
AZPS	2014	Blade origin (irradiance)	13.02	0.0013**
AZPS	2014	Light	6.47	0.0173*
AZPS	2014	Flow velocity	0.68	0.4164
AZPS	2014	Blade origin × flow velocity	5.61	0.0256*
PS	2015	pCO_2	10.08	0.0035**
PS	2015	Blade origin (wave exposure)	7.85	0.0088**
PS	2015	Light	12.75	0.0012**
PS	2015	Flow velocity	76.31	<0.0001***
PS	2015	Blade origin × flow velocity	0.16	0.6908
AZPS	2015	pCO_2	12.52	0.0013**
AZPS	2015	Blade origin (wave exposure)	4.37	0.0451*
AZPS	2015	Light	0.41	0.529
AZPS	2015	Flow velocity	9.29	0.0048**
AZPS	2015	Blade origin × flow velocity	0.21	0.6536

In 2015, samples from low wave exposure habitats demonstrated increased photosynthesis ($P = 0.0088$) and AZPS ($P = 0.0451$) relative to those from high

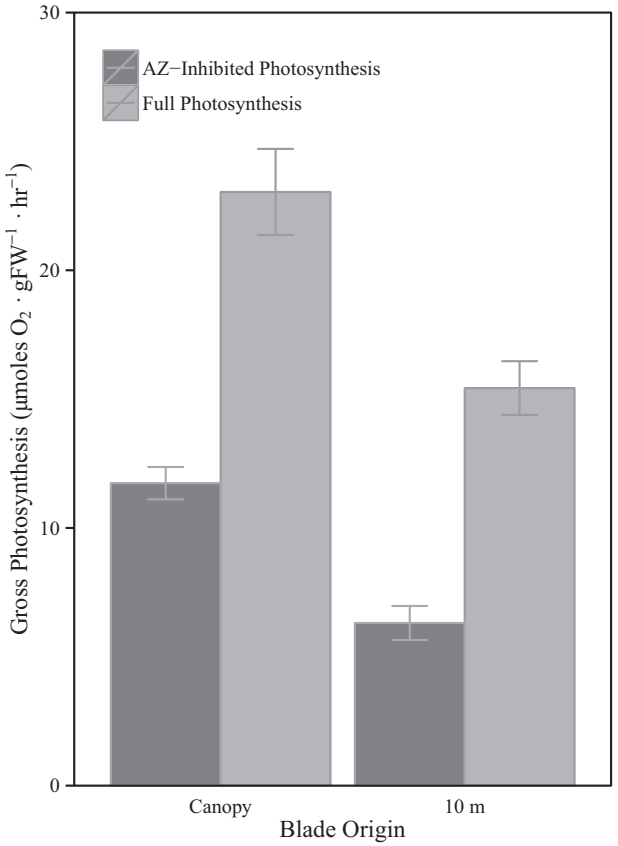

FIG. 4. Gross photosynthetic rate of uninhibited photosynthesis and AZ-inhibited photosynthesis (AZPS) grouped by blade origin (surface and 10 meter depth). Each bar represents four replicate trials. Error bars represent SE. Data are from the high irradiance treatment only (1,000 μmols photons · m^{-2}) in the 2015 experiment.

wave exposure habitats, but there was no interaction with flow velocity treatments (ANOVA, Table 2). This result, however, is likely a Type I error. The significance is driven by high photosynthesis in a single treatment cross (low exposure origin, high irradiance, high velocity), and is likely a site effect of high photosynthesis rates in blades from the Breakwater and Hopkins Marine Station. pCO_2 was strongly correlated with photosynthesis rates ($P = 0.0035$) and AZPS rates ($P = 0.0013$).

No differences were detected in the above treatments when normalized either to blade wet weight or total pigment concentration. Photosynthetic rates of long incubation duration (5–6 d) did not significantly decrease relative to mid (3–4 d) or short incubation duration (1–2 d) as measured in oxygen evolution trials in 2014 (Least Squares Means Contrast, $P = 0.8968$) or in 2015 (LSMC, $P = 0.8969$). R2 was significantly greater than R1 in 2014 (*t*-test: $t_{60} = -2.89$, $P = 0.0053$), indicating possible thermal stress or osmotic shock during oxygen evolution (Lapointe et al. 1984, Henkel and Hofmann 2008). In 2015, however, R2 and R1 were not significantly different (*t*-test: $t_{63.8} = 1.15$, $P = 0.2541$). Overall, respiration rates remained low during oxygen evolution trials. In 2014, the average ratio of PS:R1 was 18.45 ± 3.23; in 2015, the average ratio of PS: R1 was 12.41 ± 2.33 (see Fig. S4 for graphical representation of PS vs. AZPS vs. R1 vs. R2).

Relative pigment concentrations of experimental samples. In 2014, blades from 10 m depth at McAbee had a higher ratio of fucoxanthin to chl *a* (0.62 ± 0.021) than surface blades (0.51 ± 0.024, *t*-test, $P = 0.0008$), supporting the possibility that the two blade types possess acclimated photosynthetic physiology to their respective microhabitats. Pigment composition was not related to incubation duration of each blade (least squares mean contrast test); however, we lack pigment composition data prior to the incubation, so there is still the possibility of an incubation effect. In 2015, there were no significant differences between the pigment compositions of surface blades collected from different sites or exposure categories. The average ratio of fuc:Chl *a* in blades collected in 2015 was 0.5 ± 0.05. Additional pigment data for both years are given in Table 3.

DISCUSSION

Our results are the first to demonstrate that patterns of EBU-supported photosynthesis in *M. pyrifera* are influenced by irradiance and flow velocity. In both experiments, high irradiance increased the proportion of photosynthesis supported by external bicarbonate use. In the field, this means that canopy

TABLE 3. Mean (± one SD) grams of pigment (chl *a*, fucoxanthin, and chl *c*) per gram of fresh *Macrocystis pyrifera* tissue. In 2014, blade tissue was sampled at the surface and at depth (10 m) at McAbee. In 2015, blade tissue was sampled from the surface from three protected (low wave exposure) and three exposed (high wave exposure) sites.

Blade origin	g Chl *a* · g^{-1} FW	g fx · g^{-1} FW	g Chl *c* · g^{-1} FW	Fuc:Chl *a* (by mass)	Year sampled	Habitat
McAbee (surface)	0.32 ± 0.070	0.16 ± 0.028	0.063 ± 0.015	0.51 ± 0.094	2014	Protected
McAbee (10 m)	0.30 ± 0.064	0.18 ± 0.033	0.095 ± 0.015	0.62 ± 0.084	2014	Protected
Sunset Pt.	0.20 ± 0.037	0.084 ± 0.029	0.037 ± 0.010	0.41 ± 0.057	2015	Exposed
Pt. Pinos	0.20 ± 0.051	0.10 ± 0.052	0.046 ± 0.023	0.47 ± 0.17	2015	Exposed
Otter Point	0.25 ± 0.065	0.12 ± 0.033	0.060 ± 0.019	0.52 ± 0.11	2015	Exposed
Hopkins	0.27 ± 0.14	0.12 ± 0.084	0.056 ± 0.043	0.44 ± 0.086	2015	Protected
McAbee	0.19 ± 0.088	0.086 ± 0.051	0.041 ± 0.023	0.43 ± 0.12	2015	Protected
Stillwater	0.21 ± 0.062	0.10 ± 0.050	0.047 ± 0.021	0.49 ± 0.14	2015	Protected

blades likely utilize significantly more bicarbonate than light-limited blades at depth. Contrary to our hypotheses, however, decreasing flow velocity below a saturation threshold greatly *decreased* the proportion of external bicarbonate use in *M. pyrifera* blades. Kelp blades experiencing flows below 3 cm $\cdot$ s^{-1} used, on average, 30% less EBU to support PS than blades experiencing flows of 10 cm $\cdot$ s^{-1}. This indicates that EBU is not stimulated by limiting [Ci], but is rather a passive function if Ci supply. It is certainly possible that active (ion exchange channel-mediated) bicarbonate utilization, which we did not measure in this study, may respond to limiting [Ci]; this requires further work.

Most studies that have observed photosynthetic limitation of aquatic autotrophs at low flow velocities (0–3 cm $\cdot$ s^{-1}) attribute this pattern to nutrient limitation; very low flows generate thick boundary layers through which Ci and other nutrients must diffuse, potentially restricting productivity (Koehl and Alberte 1988, Nishihara and Ackerman 2009). Another mechanism has been proposed, however, in which the diffusive boundary layer may restrict efflux of O_2, resulting in high extracellular oxygen concentrations. O_2 retention could then restrict photosynthesis by promoting photorespiration or the production of reactive oxygen species (Mass et al. 2010). Flow velocity treatments in 2014 did not impact the proportion of EBU, but this is likely because nutrient influx/efflux as a function of boundary layer thickness is maximized at velocities greater than 3 cm $\cdot$ s^{-1} (Wheeler 1980, Hansen et al. 2011). While it is already clear that canopy-forming kelps locally increase seawater pH as they photosynthesize during the day, especially in the upper portion of the water column (Delille et al. 2009, Britton et al. 2016), this study adds yet another example of how *M. pyrifera* may chemically structure and stratify the water column via changes in carbon uptake physiology.

The second finding of this work is the lack of EBU acclimation in different tissues in *M. pyrifera*. In both irradiance treatments canopy blades and deep blades utilized the same percentage of bicarbonate via external catalysis (Table 1). In all other respects, however, canopy blades and deep blades exhibited expected photosynthetic acclimation. Light-replete canopy blades at McAbee possess a lower ratio of accessory pigments (fucoxanthin and chl *c*) relative to chl *a* than deep light-limited blades, as has been observed in *M. pyrifera* in Southern California and Chile (Smith and Melis 1987, Colombo-Pallotta et al. 2006). Our data also corroborate the finding that light-limited blades possess significantly lower photosynthetic rates than light-replete blades in Southern Californian and Chilean populations of *M. pyrifera* (Arnold and Manley 1985, Smith and Melis 1987, Colombo-Pallotta et al. 2006); this pattern has been attributed to the greater efficiency and photosystem turnover in light-acclimated blades. In our study, this observation may also have been due to photoinhibition in blades from deep waters, which were likely not acclimated to the high irradiance to which they were subjected. Regardless, there is no evidence that deep and canopy blades differ in their carbon uptake dynamics. This result supports the conclusion that *M. pyrifera* tissue does not up-regulate EBU in response to limiting [Ci].

Across all years and treatments, we find that *M. pyrifera* in the Monterey Bay utilize bicarbonate via external catalysis to support an average 40% of PS, corroborating the findings of Brown et al. (2014). The remaining 60% of photosynthesis is supported by dissolved CO_2 and an unknown proportion of active bicarbonate uptake via ion exchange proteins. This finding differs from the report that *M. pyrifera* from New Zealand use less than 20% external bicarbonate uptake at pH 7.65 (Fernández et al. 2014). Our experiments were carried out in seawater of varying pH, which prevents direct comparison to the more controlled approach of Fernandez et al. It is, however, remotely possible that there is a genetic divergence between carbon uptake in northern and southern hemisphere populations of *M. pyrifera*. Although *M. pyrifera* is a monotypic species (Coyer et al. 2001), strong ecotypic variation has been observed in holdfast, habit, and blade morphology (e.g., *integrifolia* vs. *pyrifera* morphs). On the California coast, for example, local adaptation of nitrate uptake physiology in different populations of *M. pyrifera* has occurred despite the fact these populations likely still exchange genetic material via long-distance dispersal (Kopczak et al. 1991).

The results of this research indicate that utilization of different Ci species (CO_2 and bicarbonate) is a plastic process regulated by persistent abiotic variables in the nearshore marine system. This work contributes to our understanding of not only the impact of the abiotic environment on *M. pyrifera*, but also give us a sense of how *M. pyrifera* may in turn structure carbonate chemistry in kelp forest microhabitats.

The authors sincerely thank Erick Sturm and the NOAA Southwest Fisheries Science Center for providing access to a Loligo respirometer, as well as support and infrastructure. Brian Gaylord provided the use of the Acoustic Doppler Current Profiler. We thank Mark Carr, Pete Raimondi, and Jarmila Pittermann for critical feedback on the manuscript. We also thank Jose Ayala and Zachary Benavidez for dedicated lab work and experimental assistance. Funding for this work was provided by an NSF GRFP awarded to STD, an NSF REU awarded to CM, the Phycological Society of America, and the Earl and Ethel Myers Oceanographic Trust. The authors declare no conflict of interest.

Alonso Vega, J. M., Vásquez, J. A. & Buschmann, A. H. 2005. Population biology of the subtidal kelps *Macrocystis integrifolia* and *Lessonia trabeculata* (Laminariales, Phaeophyceae) in an upwelling ecosystem of northern Chile: interannual variability and El Niño 1997-1998. *Rev. Chil. Hist. Nat.* 78:33–50.

Arnold, K. E. & Manley, S. L. 1985. Carbon allocation in *Macrocystis pyrifera* (Phaeophyta): intrinsic variability in photosynthesis and respiration. *J. Phycol.* 21:154–67.

Britton, D., Cornwall, C. E., Revill, A. T., Hurd, C. L. & Johnson, C. R. 2016. Ocean acidification reverses the positive effects of seawater pH fluctuations on growth and photosynthesis of the habitat-forming kelp, *Ecklonia radiata*. *Sci. Rep.* 6:26036.

Brostoff, W. 1988. Taxonomic studies of *Macrocystis pyrifera* (L.) C. Agardh (Phaeophyta) in Southern California: holdfasts and basal stipes. *Aquat. Bot.* 31:289–305.

Brown, M. B., Edwards, M. S. & Kim, K. Y. 2014. Effects of climate change on the physiology of giant kelp, *Macrocystis pyrifera*, and grazing by the purple sea urchin, *Strongylocentrotus purpuratus*. *Algae* 29:203–15.

Cabello-Pasini, A., Aguirre-Von-Wobeser, E. & Figueroa, F. L. 2000. Photoinhibition of photosynthesis in *Macrocystis pyrifera* (Phaeophyceae), *Chondrus crispus* (Rhodophyceae) and *Ulva lactuca* (Chlorophyceae) in outdoor culture systems. *J. Photochem. Photobiol. B Biol.* 57:169–78.

Carr, M. H. & Reed, D. C. 2016. Shallow rocky reefs and kelp forests. *In* Mooney, H. & Zavaleta, E. S. [Eds.] *Ecosystems of California*. University of California Press, Berkeley, California, pp. 311–36.

Colombo-Pallotta, M. F., García-Mendoza, E. & Ladah, L. B. 2006. Photosynthetic performance, light absorption, and pigment composition of *Macrocystis Pyrifera* (Laminariales, Phaeophyceae) blades from different depths. *J. Phycol.* 42:1225–34.

Coyer, J. A., Smith, G. J. & Andersen, R. A. 2001. Patterns of *Macrocystis pyrifera* (Phaeophyceae) evolution and biogeography as determined by ITS1 and ITS2 sequences. *J. Phycol.* 37:574–85.

Dayton, P. 1972. Toward an understanding of community resilience and the potential effects of enrichments to the benthos at McMurdo Sound, Antarctica. *In* Parker, B. [Ed.] *Proceedings of the Colloquium on Conservation Problems in Antarctica*. Allen Press, Lawrence, Kansas, pp. 81–96.

Delille, B., Borges, A. V. & Delille, D. 2009. Influence of giant kelp beds (*Macrocystis pyrifera*) on diel cycles of pCO_2 and DIC in the Sub-Antarctic coastal area. *Estuar. Coast. Shelf Sci.* 81:114–22.

Drake, P. T., McManus, M. A. & Storlazzi, C. D. 2005. Local wind forcing of the Monterey Bay area inner shelf. *Cont. Shelf Res.* 25:397–417.

Drechsler, Z., Sharkia, R., Cabantchik, Z. I. Z. & Beer, S. 1993. Bicarbonate uptake in the marine macroalga *Ulva* sp. is inhibited by classical probes of anion exchange by red blood cells. *Planta* 191:34–40.

Edwards, M. S. 1998. Effects of long-term kelp canopy exclusion on the abundance of the annual alga *Desmarestia ligulata* (Light F). *J. Exp. Mar. Bio. Ecol.* 228:309–26.

Edwards, M. S. & Kim, K. Y. 2010. Diurnal variation in relative photosynthetic performance in giant kelp *Macrocystis pyrifera* (Phaeophyceae, Laminariales) at different depths as estimated using PAM fluorometry. *Aquat. Bot.* 92:119–28.

Ellison, A. M., Bank, M. S., Clinton, B. D., Colburn, E. A., Elliott, K., Ford, C. R., Foster, D. R. et al. 2005. Loss of foundation species: consequences for the structure and dynamics of forested ecosystems. *Front. Ecol. Environ.* 3:479–86.

Erikson, L., Storlazzi, C. & Golden, N. 2014. Wave height, peak period, and orbital velocity for the California continental shelf. U.S. Geological Survey data set.

Fernández, P., Hurd, C. L. & Roleda, M. Y. 2014. Bicarbonate uptake via an ion exchange protein is the main mechanism of inorganic carbon acquisition by the giant kelp *Macrocystis pyrifera* (Laminariales, Phaeophyceae) under variable pH. *J. Phycol.* 50:998–1008.

Fernández, P., Roleda, M. Y. & Hurd, C. L. 2015. Effects of ocean acidification on the photosynthetic performance, carbonic anhydrase activity and growth of the giant kelp *Macrocystis pyrifera*. *Photosynth. Res.* 124:293–304.

Figurski, J. 2010. *Patterns and Sources of Variation in Drift Algae and the Ecological Consequences for Kelp Forests*. University of California, Santa Cruz, Santa Cruz, California.

Frieder, C. A., Nam, S. H., Martz, T. R. & Levin, L. A. 2012. High temporal and spatial variability of dissolved oxygen and pH in a nearshore California kelp forest. *Biogeosciences* 9:3917–30.

Gaylord, B., Denny, M. W. & Koehl, M. A. R. 2003. Modulation of wave forces on kelp canopies by alongshore currents. *Limnol. Oceanogr.* 48:860–71.

Gerard, V. A. 1982. Growth and utilization of internal nitrogen reserves by the giant kelp *Macrocystis pyrifera* in a low-nitrogen environment. *Mar. Biol.* 66:27–35.

Gerard, V. A. 1984. The light environment in a giant kelp forest: influence of *Macrocystis pyrifera* on spatial and temporal variability. *Mar. Biol.* 84:189–95.

Graham, M. H., Harrold, C., Lisin, S., Light, K., Watanabe, J. M. & Foster, M. S. 1997. Population dynamics of giant kelp *Macrocystis pyrifera* along a wave exposure gradient. *Mar. Ecol. Prog. Ser.* 148:269–279.

Graham, M. H., Vasquez, J. A. & Buschmann, A. H. 2007. Global ecology of the giant kelp *Macrocystis*: from ecotypes to ecosystems. *Oceanography and Marine Biology*. 45: p. 39–88.

Hansen, A. T., Hondzo, M. & Hurd, C. L. 2011. Photosynthetic oxygen flux by *Macrocystis pyrifera*: a mass transfer model with experimental validation. *Mar. Ecol. Prog. Ser.* 434:45–55.

Henkel, S. K. & Hofmann, G. E. 2008. Thermal ecophysiology of gametophytes cultured from invasive *Undaria pinnatifida* (Harvey) Suringar in coastal California harbors. *J. Exp. Mar. Bio. Ecol.* 367:164–73.

Hennon, G. M. M., Ashworth, J., Groussman, R. D., Berthiaume, C., Morales, R. L., Baliga, N. S., Orellana, M. V. et al. 2015. Diatom acclimation to elevated CO_2 via cAMP signalling and coordinated gene expression. *Nat. Clim. Chang.* 5:761–6.

Hurd, C. L. & Pilditch, C. A. 2011. Flow-induced morphological variations affect diffusion boundary-layer thickness of *Macrocystis pyrifera* (Heterokontophyta, Laminariales). *J. Phycol.* 47:341–51.

Johnston, A. M. & Raven, J. A. 1990. Effects of culture in high CO_2 on the photosynthetic physiology of *Fucus serratus*. *Eur. J. Phycol.* 25:75–82.

Jones, C., Lawton, J. & Shachak, M. 1994. Organisms as ecosystem engineers. *Oikos* 69:373–86.

Kapsenberg, L. & Hofmann, G. E. 2016. Ocean pH time-series and drivers of variability along the northern Channel Islands, California, USA. *Limnol. Oceanogr.* 61:3:953–68.

Klenell, M., Snoeijs, P. & Pedersén, M. 2004. Active carbon uptake in *Laminaria digitata* and *L. saccharina* (Phaeophyta) is driven by a proton pump in the plasma membrane. *Hydrobiologia* 514:41–53.

Koehl, M. A. R. & Alberte, R. R. S. 1988. Flow, flapping, and photosynthesis of *Nereocystis luetkeana*: a functional comparison of undulate and flat blade morphologies. *Mar. Biol.* 99:435–44.

Kopczak, C. D., Zimmerman, R. C. & Kremer, J. N. 1991. Variation in nitrogen physiology and growth among geographically isolated populations of the giant kelp, *Macrocystis pyrifera* (Phaeophyta). *J. Phycol.* 27:149–58.

Koweek, D. A., Nickols, K. J., Leary, P. R., Litvin, S. Y., Bell, T. W., Luthin, T., Lummis, S., Mucciarone, D. A., and Dunbar, R. B. 2016. A year in the life of a central California kelp forest: physical and biological insights into biogeochemical variability. Biogeosciences Discuss. in review.

Kubler, J. E. & Raven, J. A. 1995. The interaction between inorganic carbon acquisition and light supply in Palmaria Palmata (Rhodophyta). *J. Phycol.* 31:369–75.

Lapointe, B. E., Rice, D. L. & Lawrence, J. M. 1984. Responses of photosynthesis, respiration, growth and cellular constituents to hypo-osmotic shock in the red alga *Gracilaria tikvahiae*. *Comp. Biochem. Physiol. Part A Physiol.* 77:127–32.

Larsson, C. & Axelsson, L. 1999. Bicarbonate uptake and utilization in marine macroalgae. *Eur. J. Phycol.* 34:79–86.

Mass, T., Genin, A., Shavit, U., Grinstein, M. & Tchernov, D. 2010. Flow enhances photosynthesis in marine benthic autotrophs by increasing the efflux of oxygen from the organism to the water. *Proc. Natl. Acad. Sci. USA* 107:2527–31.

Mcginn, P. J., Price, G. D. & Badger, M. R. 2004. High light enhances the expression of low-CO_2-inducible transcripts

involved in the CO_2-concentrating mechanism in *Synechocystis sp.* PCC6803. *Plant, Cell Environ.* 27:615–26.
Mercado, J. M., Andría, J. R., Pérez-Llorens, J. L., Vergara, J. J. & Axelsson, L. 2006. Evidence for a plasmalemma-based CO_2 concentrating mechanism in *Laminaria saccharina*. *Photosynth. Res.* 88:259–68.
Nishihara, G. N. & Ackerman, J. D. 2009. Diffusive boundary layers do not limit the photosynthesis of the aquatic macrophyte, *Vallisneria americana*, at moderate flows and saturating light levels. *Limnol. Oceanogr.* 54:1874–82.
Pierrot, D., Lewis, E. & Wallace, D. 2006. MS excel program developed for CO_2 system calculations. ORNL/CDIAC-105a.
Raven, J. A., Beardall, J. & Giordano, M. 2014. Energy costs of carbon dioxide concentrating mechanisms in aquatic organisms. *Photosynth. Res.* 121:111–24.
Raven, J. A. & Hurd, C. L. 2012. Ecophysiology of photosynthesis in macroalgae. *Photosynth. Res.* 113:105–25.
Schiel, D. R. & Foster, M. S. 2015. *The Biology and Ecology of Giant Kelp Forests*. University of California Press, Oakland, CA.
Seely, G., Duncan, M. & Vidaver, W. 1972. Preparative and analytical extraction of pigments from brown algae with dimethyl sulfoxide. *Mar. Biol.* 12:184–8.
Sharkey, T. D., Stitt, M., Heineke, D., Gerhardt, R., Raschke, K. & Heldt, H. W. 1986. Limitation of photosynthesis by carbon metabolism II. O_2-insensistive CO_2 uptake results from limitation of triose phosphate utilization. *Plant Physiol.* 81:1123–9.
Smith, B. M. & Melis, A. 1987. Photosystem stoichiometry and excitation distribution in chloroplasts from surface and minus 20 meter blades of *Macrocystis pyrifera*, the giant kelp. *Plant Physiol.* 84:1325–30.
Stewart, H. L., Fram, J. & Reed, D. C. 2009. Differences in growth, morphology and tissue carbon and nitrogen of *Macrocystis pyrifera* within and at the outer edge of a giant kelp forest in California, USA. *Mar. Ecol. Prog. Ser.* 375:101–12.
Storlazzi, C., McManus, M. & Figurski, J. 2003. Long-term, high-frequency current and temperature measurements along central California: insights into upwelling/relaxation and internal waves on the inner shelf. *Cont. Shelf Res.* 23:901–18.
The Royal Society. 2005. Ocean acidification due to increasing atmospheric carbon dioxide.
Utter, B. & Denny, M. W. 1996. Wave-induced forces on the giant kelp *Macrocystis pyrifera* (Agardh): field test of a computational model. *J. Exp. Biol.* 199:2645–54.
Ward, B. B. 2005. Temporal variability in nitrification rates and related biogeochemical factors in Monterey Bay, California, USA. *Mar. Ecol. Prog. Ser.* 292:97–109.
Wheeler, W. N. 1980. Effect of boundary layer transport on the fixation of carbon by the giant kelp *Macrocystis pyrifera*. *Mar. Biol.* 56:103–10.
Woodson, C. B., Eerkes-Medrano, D. I., Flores-Morales, A., Foley, M. M., Henkel, S. K., Hessing-Lewis, M., Jacinto, D. et al. 2007. Local diurnal upwelling driven by sea breezes in northern Monterey Bay. *Cont. Shelf Res.* 27:2289–302.
Young, J., Kranz, S., Goldman, J., Tortell, P. & Morel, F. 2015. Antarctic phytoplankton down-regulate their carbon-concentrating mechanisms under high CO_2 with no change in growth rates. *Mar. Ecol. Prog. Ser.* 532:13–28.
Zou, D., Gao, K. & Xia, J. 2003. Photosynthetic utilization of inorganic carbon in the economic brown alga, *Hizikia fusiforme* (Sargassaceae) from the South China Sea. *J. Phycol.* 39:1095–100.

Supporting Information

Additional Supporting Information may be found in the online version of this article at the publisher's web site:

Figure S1. Irradiance spectrum of wavelengths emitted by the combination of a blue bulb and sodium halide lamp during oxygen evolution trials.

Table S1 Decimal bearing, wave-exposure classification, and annual orbital wave velocity for each collection site.

Figure S2. Boxplot of (A) measurements of pCO_2 of experimental seawater for 16 trials in the 2014 experiment and all trials in the 2015 experiment and (B) measurements of pH during of experimental seawater for 16 trials in the 2014 experiment and all trials in the 2015 experiment.

Figure S3. Percentages of 15 min periods (A, B) and 60 min periods (C, D) each day in October when velocities were less than or equal to 3 cm $\cdot$ s^{-1} (blue), between 3 and 10 cm $\cdot$ s^{-1} (teal) or greater than 10 cm $\cdot$ s^{-1} (yellow) at the closest ADCP bin to the bottom (1.5 m above bottom; A, C) and the closest ADCP bin to the surface (8.5 m above bottom; B, D).

Figure S4. Average oxygen evolution rates for the four measurement phases (full photosynthesis (PS), acetazolamide-inhibited photosynthesis (AZPS), respiration period 1 (R1), and respiration period 2 (R2) for all trials over two measurement years (2014 and 2015). Error bars represent standard error.

Figure S5. Gross photosynthetic rate of full (uninhibited photosynthesis, PS) and AZ-inhibited photosynthesis (AZPS) as a function of PAR level (1,000 or 80 μmol photons $\cdot$ m^{-2} $\cdot$ s^{-1}) and blade depth (surface and 10 m depth).

Figure S6. Gross photosynthetic rate of full (uninhibited photosynthesis, PS) and AZ-inhibited photosynthesis (AZPS) as a function of PAR level (800 or 100 μmol photon $\cdot$ m^{-2} $\cdot$ s^{-1}) and flow velocity (3 and 10 cm $\cdot$ s^{-1}).